Sound quality assessment of wood for xylophone bars

Mitsuko Aramaki[a)]
CNRS Laboratoire de Mécanique et d'Acoustique 31, chemin Joseph Aiguier 13402 Marseille Cedex 20, France

Henri Baillères and Loïc Brancheriau
CIRAD-Forêt, TA 10/16, avenue Agropolis, 34398 Montpellier Cedex 5, France

Richard Kronland-Martinet and Sølvi Ystad
CNRS, Laboratoire de Mécanique et d'Acoustique 31, chemin Joseph Aiguier 13402 Marseille Cedex 20, France

(Received 15 March 2006; revised 22 January 2007; accepted 22 January 2007)

Xylophone sounds produced by striking wooden bars with a mallet are strongly influenced by the mechanical properties of the wood species chosen by the xylophone maker. In this paper, we address the relationship between the sound quality based on the timbre attribute of impacted wooden bars and the physical parameters characterizing wood species. For this, a methodology is proposed that associates an analysis-synthesis process and a perceptual classification test. Sounds generated by impacting 59 wooden bars of different species but with the same geometry were recorded and classified by a renowned instrument maker. The sounds were further digitally processed and adjusted to the same pitch before being once again classified. The processing is based on a physical model ensuring the main characteristics of the wood are preserved during the sound transformation. Statistical analysis of both classifications showed the influence of the pitch in the xylophone maker judgement and pointed out the importance of two timbre descriptors: the frequency-dependent damping and the spectral bandwidth. These descriptors are linked with physical and anatomical characteristics of wood species, providing new clues in the choice of attractive wood species from a musical point of view. © *2007 Acoustical Society of America.* [DOI: 10.1121/1.2697154]

PACS number(s): 43.75.Kk, 43.66.Jh, 43.60.Uv [NFH] Pages: 2407–2420

I. INTRODUCTION

The mechanical and anatomical properties of woods are of importance for the sound quality of musical instruments. Yet, depending on the role of the wooden elements, these properties may differ. Xylophone sounds are produced by striking wooden bars with a mallet, and thus the mechanical properties of the wood are important. This study is the first step towards understanding what makes the sound of an impacted wooden bar attractive for xylophone makers from a musical point of view. For this purpose, we recorded sounds from a wide variety of wood species to compare their sound quality and relate it to the wood properties. An original methodology is proposed that associates analysis-synthesis processes and perceptual classification analysis. Perceptual classification was performed by a renowned instrument maker.

The xylophone maker community agrees on the choice of wood species. This choice is driven by the sound quality, but other nonacoustically relevant properties are considered as well (e.g., robustness; esthetic aspects). The wood species most used in xylophone manufacturing is *Dalbergia* sp. Several authors have sought to determine which physical characteristics are of importance for the generated sound. In particular, Holz (1996) concluded that an "ideal" xylophone wood bar is characterized by a specific value range of density, Young modulus, and damping factors. Ono and Norimoto (1983) demonstrated that samples of spruce wood (*Picea excelsa, P. glehnii, P. sitchensis*)—considered a suitable material for soundboards—all had a high sound velocity and low longitudinal damping coefficient as compared to other softwoods. The cell-wall structure may account for this phenomenon. Internal friction and the longitudinal modulus of elasticity are markedly affected by the microfibril angle in the S2 tracheid cell layer, but this general trend does not apply to all species. For instance, pernambuco (*Guilandina echinata* Spreng.), traditionally used for making violin bows, has an exceptionally low damping coefficient relative to other hardwoods and softwoods with the same specific modulus (Bucur, 1995; Matsunaga *et al.*, 1996; Sugiyama *et al.*, 1994). This feature has been explained by the abundance of extractives in this species (Matsunaga and Minato, 1998). Obataya *et al.*(1999) confirmed the importance of extractives for the rigidity and damping qualities of reed materials. Matsunaga *et al.* (1999) reduced the damping coefficient of spruce wood by impregnating samples with extractives of pernambuco (*Guilandina echinata* Spreng.). The high sound quality conditions are met by the wood species commonly used by xylophone makers (like *Dalbergia* sp.), but other tropical woods may serve. We propose to focus on the perceptual properties of impacted wood bars as the basis for pointing out woods suitable for xylophone manufacturing. Several studies using natural or synthetic sounds have been conducted to point out auditory clues associated with geom-

[a)]Author to whom correspondence should be addressed. Electronic mail: aramaki@lma.cnrs-mrs.fr

etry and material properties of vibrating objects (Avanzini and Rocchesso, 2001; Giordano and McAdams, 2006; Lutfi and Oh, 1997; Klatzky *et al.*, 2000; McAdams *et al.*, 2004). These studies revealed the existence of perceptual clues allowing the source of the impact sound to be identified merely by listening. In particular, the perception of material correlated mainly with the internal friction (related to the damping factors of the spectral components) as theoretically shown by Wildes and Richards (1988). Nevertheless, it has not been determined whether the perceptual clues highlighted in the distinction of different materials are those used to establish the subjective classification of different species of wood.

The perceptual differences reported in the literature are linked with subtle changes in timbre, defined as "the perceptual attribute that distinguishes two tones of equal, pitch, loudness, and duration" (ANSI, 1973). This definition points out the importance of comparing sounds with similar loudness, duration, and pitch. Concerning loudness and duration, the sounds of interest can easily be adjusted in intensity by listening, and they have about the same duration since they correspond to the very narrow category of impacted wooden bars. Concerning pitch, the bars do not have the same values because the pitch depends on the physical characteristics of the wood, i.e., essentially of the Young modulus and the mass density. To tune the sounds to the same pitch, we propose to digitally process the sounds recorded on bars of equal length. Synthesis models can be used for this purpose, allowing virtual tuning by altering the synthesis parameters. Such an approach combining sound synthesis and perceptual analysis has already been proposed. Most of the proposed models are based on the physics of vibrating structures, leading to a modal approach of the synthesis process (Adrien, 1991; Avanzini and Rocchesso, 2001) or to a numerical method of computation (Bork, 1995; Chaigne and Doutaut, 1997; Doutaut *et al.*, 1998). Yet, although these models lead to realistic sounds, they do not easily allow for an analysis-synthesis process implicating the generation of a synthetic sound perceptually similar to an original one. To overcome this drawback, we propose an additive synthesis model based on the physics of vibrating bars, the parameters of which can be estimated from the analysis of natural sounds.

The paper is organized as follows: in Sec. II, we discuss the design of an experimental sound data bank obtained by striking 59 wooden bars made of different woods carefully selected and stabilized in a climatic chamber. In Sec. III, we then address the issue of digitally tuning the sounds without changing the intrinsic characteristics of the wood species. This sound manipulation provided a tuned sound data bank in which each sound was associated with a set of descriptors estimated from both physical experiments and signal analysis. The experimental protocol is described in Sec. IV. It consists of the classification carried by a professional instrument maker. The classification was performed with both the original and the tuned data banks to better understand the influence of pitch on the classification. These results are discussed in Sec. VII, leading to preliminary conclusions that agree with most of the knowledge and usage in both wood mechanics, xylophone manufacturing, and sound perception.

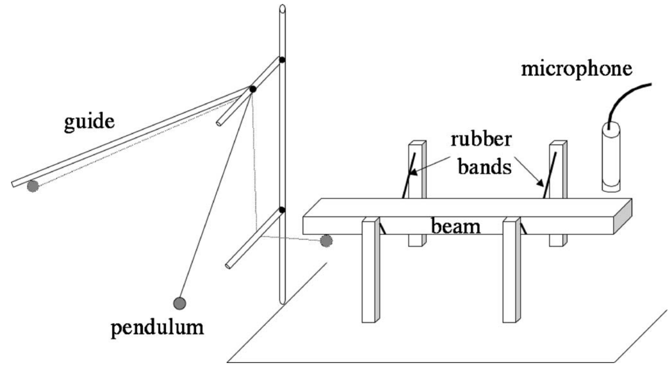

FIG. 1. Experimental setup used to strike the wood samples and record the impact sounds. The setup was placed in an anechoic room.

II. DESIGN OF AN EXPERIMENTAL SOUND DATA BANK

a. Choice of wood species. Most percussive instruments based on wooden bars are made of specific species (for example, *Dalbergia* sp. or *Pterocarpus* sp.). In this experiment, we used tropical and subtropical species, most of which were unknown to instrument makers. A set of 59 species presenting a large variety of densities (from 206 to 1277 kg/m^3) were chosen from the huge collection (about 8000) of the CIRAD (Centre de coopération Internationale en Recherche Agronomique pour le Développement, Montpellier, France). Their anatomical and physical characteristics have been intensely studied and are well described. The name and density of each species are in Table III.

b. Manufacturing wooden bars. Both geometry and boundary conditions govern the vibration of bars. By considering bars with the same geometry and boundary conditions, sounds can be compared to determine the intrinsic quality of the species. Hence, a set of bars was made according to the instrument maker recommendations. The bars were manufactured to be as prismatic as possible, with dimensions $L = 350\ mm \times W = 45\ mm \times T = 20\ mm$, without singularities and cut in the grain direction. We assume that the growth rings are parallel to the tangential wood direction and that their curvature is negligible. The longitudinal direction is collinear to the longitudinal axis of the bars. The bars were stabilized in controlled conditions.

c. Recording of impact sounds under anechoic conditions. An experimental setup was designed that combines an easy way to generate sounds with a relative precision ensuring the repeatability of the measurements, as shown in Fig. 1. In this way, impact excitation was similar for all the impacted bars. Moreover, to minimize the sound perturbations due to the environment, the measurements took place in an anechoic room.

The bar was placed on two rubber bands, ensuring free-free-type boundary conditions. The rubbers minimized perturbations due to suspension (see, for example, Blay *et al.*, 1971 for more details). Bars were struck with a small steel pendulum. The ball on the string was released from a constrained initial position (guide), and after the string wrapped around a fixed rod, the ball struck the bar from underneath. The robustness of this simple procedure showed the radiated sounds were reproducible: the determination error was less than 0.1% for the fundamental frequency and 4.3% for the damping coefficient of the first mode (Brancheriau *et al.*, 2006a). To ensure broad spectral excitation, the ball was chosen to generate a sufficiently short pendulum/bar contact (to be as close as possible to an ideal Dirac source). The excitation spectrum is given by the Fourier transform of the impact force, so that the shorter the impact, the broader the spectrum excitation. For that, a steel ball was used since the modulus of elasticity of steel is much larger than that of wood (the ratio is about 200). This setup makes contact duration between the ball and the bar short (Graff, 1975). This duration was shortened because the impact point was underneath the bar, maximizing the reversion force. After several experiments, a good compromise between speed, short duration, and lack of deformation of the material was obtained with a steel ball of 12 g and a 14 mm diameter, tightened by a 30-cm-long string. The impact point played an important role in the generation of sounds. To prevent the first modes from vanishing, the bar was struck close to one of its extremities (at 1 cm), allowing high frequency modes to develop. An omni-directional microphone (Neumann KM183mt) was placed in the close sound field at the opposite end of the impact location to measure the sound-radiated pressure. This configuration obviates the contribution of the spectral peak generated by the ball, peak which was at about 10 kHz. The sounds were digitally recorded at 48 kHz sampling frequency.

d. Signal characteristics. Figure 2 shows the temporal signal, the spectral representation, and the time-frequency representation of a typical sound obtained experimentally. The temporal signals are characterized by a short onset and a fast decay. Consequently, their durations generally do not exceed 1 s. Their spectra are composed of emergent resonances that do not overlap much. As shown by the time-frequency representation, the damping of these spectral components is frequency dependent, the high frequency components being more heavily damped than the low frequency ones.

III. DESIGN OF TUNED SOUND DATA BANK FOR TIMBRE STUDY

To facilitate comparison of the timbre of sounds generated striking different wood species, their pitch was equalized. In practice, this could have been possible using the same procedure adopted by percussive instrument makers, where the bar geometry is modified removing some substance around the center of the bar to be tuned (Fletcher and Rossing, 1998). This approach comes, however, with the risk of making irreversible mistakes, for example, removing an excessive amount of wood. As an alternative, we propose to digitally tune the pitch of sounds generated striking bars of equal length. Such an approach relies on the plausible assumption that the pitch of our recorded signals is primarily determined by the frequency of the first vibrational mode. In particular, we use a sound synthesis model which allows for sound transformations that are accurate relative to the physical phenomena, as compared to other signal processing approaches such as pitch shifting.

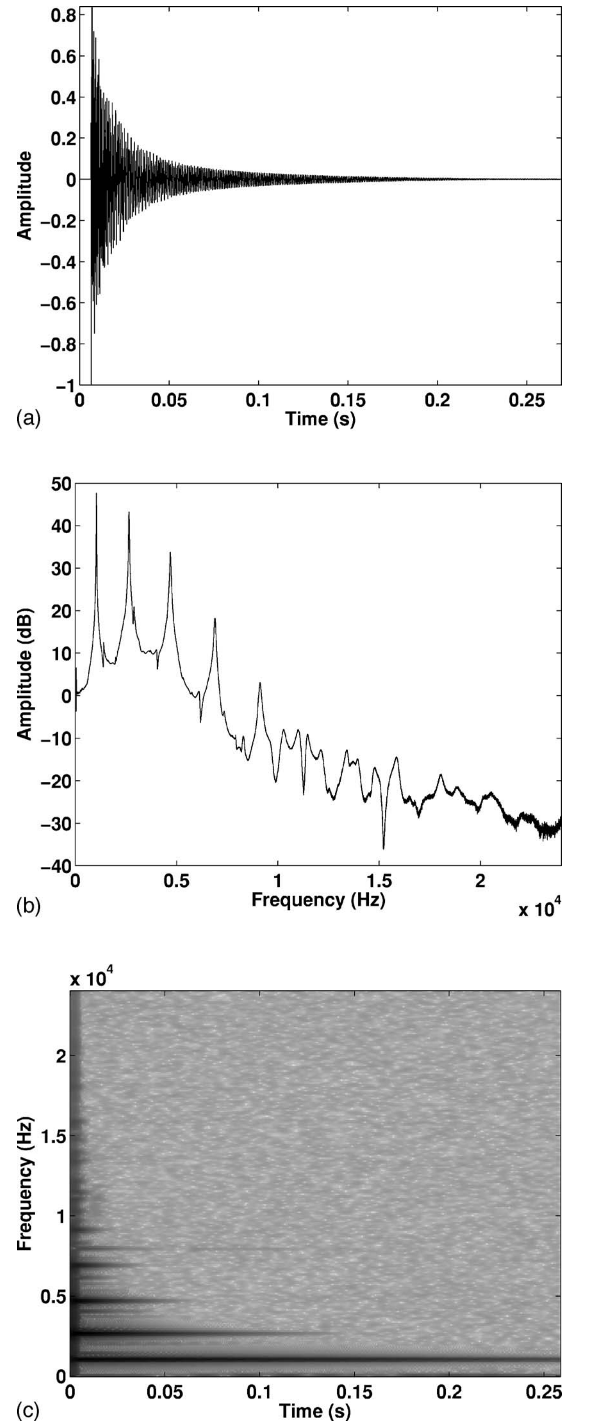

FIG. 2. (a) Wave form, (b) spectral representation, and (c) spectrogram (amplitude in logarithmic scale) of a typical sound obtained by impacting a wooden bar.

A. Synthesis model based on physical approach

To tune the sounds, we propose to use an additive synthesis model. This model simulates the main characteristics of the vibrations produced by an impacted bar to exhibit the principal properties of the radiated sound.

1. Simplified mechanical model

Numerous mechanical models of bar vibrations are available in the literature, but the relevant information can be pointed out using a simple model based on assumptions that are coherent with our experimental design. According to the manufacturing of the bars, one can assume that the fiber orientation follows the axis of the bar and that the ratio length/width is large. Consequently, one can neglect the anisotropy property of the wood and the contribution of the longitudinal and torsional modes (which are few, weak, and of little influence on the radiated sound). These assumptions allow for the consideration of a one-dimensional mechanical model depending only on the longitudinal Young modulus. Such a model can be described by the well-known Euler-Bernoulli equation

$$EI\frac{\partial^4 y(x,t)}{\partial x^4} + \rho S\frac{\partial^2 y(x,t)}{\partial t^2} = 0, \tag{1}$$

where E is the longitudinal Young modulus, I the quadratic moment, ρ the mass density, and S the cross section area. The general solution of the equation is given by

$$y(x,t) = \sum_n Y_n(x)e^{i\gamma_n t} \tag{2}$$

with

$$Y_n(x) = A\cosh(k_n x) + B\sinh(k_n x) + C\cos(k_n x) + D\sin(k_n x). \tag{3}$$

By injecting Eq. (2) and Eq. (3) into the Eq. (1), one obtains

$$\gamma_n = \pm\sqrt{\frac{EI}{\rho S}}k_n^2. \tag{4}$$

Our experimental setup corresponds to free-free boundary conditions written

$$\frac{\partial^2 Y(0)}{\partial x^2} = \frac{\partial^2 Y(L)}{\partial x^2} = \frac{\partial^3 Y(0)}{\partial x^3} = \frac{\partial^3 Y(L)}{\partial x^3} = 0$$

leading to

$$k_n = (2n+1)\frac{\pi}{2L}. \tag{5}$$

To take into account viscoelastic phenomena, E is considered as complex valued, see, for example (Valette and Cuesta, 1993)

$$E = E_d(1 + i\eta), \tag{6}$$

where E_d is the dynamical Young modulus, and η a dimensionless material loss factor. By injecting relations (5) and (6) into relation (4) and assuming that $\eta \ll 1$, one obtains the following important expressions:

$$\gamma_n = \omega_n + i\alpha_n \tag{7}$$

with

$$\begin{cases} \omega_n \approx \sqrt{\dfrac{E_d I}{\rho S}}(2n+1)^2\dfrac{\pi^2}{4L^2} \\ \alpha_n \approx \dfrac{\eta}{2}\omega_n \end{cases}. \tag{8}$$

Thus, one can rewrite the relation (2):

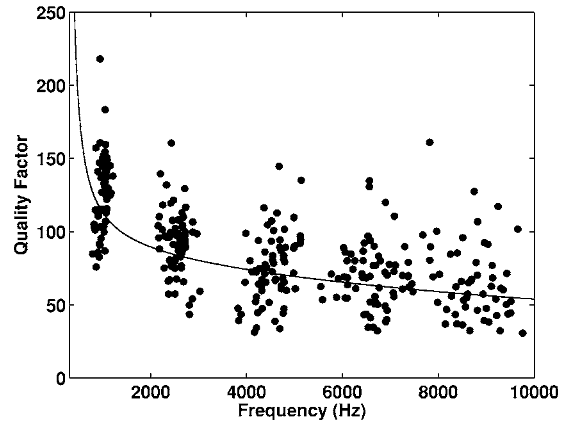

FIG. 3. Quality factor Q_n estimated on original sounds. The Q_n values are fitted, in a least squares sense, by a rational function (black curve) corresponding to Eq. (11).

$$y(x,t) = \sum_n Y_n(x)e^{i\omega_n t}e^{-\alpha_n t}. \tag{9}$$

It is accepted (Chaigne and Doutaut, 1997; McAdams *et al.*, 2004; Ono and Norimato, 1985) that the damping factors in case of wooden bars are described by a parabolic form:

$$\alpha(f) = a_0 + a_2 f^2 \tag{10}$$

where the constants a_0 and a_2 depend on the wood species. This corresponds to a quality factor Q_n given by

$$Q_n = \frac{\pi f_n}{\alpha_n} = \frac{\pi f_n}{a_0 + a_2 f_n^2}. \tag{11}$$

This behavior was experimentally verified, as shown in Fig. 3.

These expressions show that the vibrations of the bar, which are correlated with the radiated sound pressure, can be described by a sum of elementary components consisting of exponentially damped monochromatic signals. The frequency of these elementary components is inversely proportional to the square of the length of the bar, and their damping is proportional to the square of the frequency.

2. Additive synthesis model

The synthesis model aims at simulating the analytical solutions written in Eq. (9), which are expressed as a sum of exponentially damped sinusoids

$$s(x,t) = \theta(t)\sum_{n=1}^{N} A_n(x)\sin(\omega_n t)e^{-\alpha_n t}, \tag{12}$$

where N is the number of components, $\theta(t)$ the Heaviside function, A_n the amplitude, ω_n the frequency and α_n the damping coefficient of the nth component. The choice of either sine or cosine functions has no perceptual influence on the generated sounds but sine functions are often used in sound synthesis since they avoid discontinuities in the signal at $t=0$. Hence, the signal measured at a fixed location is considered to be well represented by the expression (12). Its spectral representation is given by

$$S(\omega) = \sum_{n=1}^{N} \frac{A_n}{2i} \left(\frac{1}{\alpha_n + i(\omega - \omega_n)} - \frac{1}{\alpha_n + i(\omega + \omega_n)} \right)$$

and the z transform by

$$S(z) = \sum_{n=1}^{N} \frac{A_n}{2i} \left(\frac{1}{1 - e^{(i\omega_n - \alpha_n)} z^{-1}} - \frac{1}{1 - e^{(-i\omega_n - \alpha_n)} z^{-1}} \right).$$

B. Estimation of synthesis parameters

Before the tuning process, the recorded sounds described in Sec. II are equalized in loudness, analyzed, and then resynthesized with the synthesis model described above. The loudness was equalized by listening tests. For that, the synthesis parameters are directly estimated from the analysis of the recorded sounds. The estimation of the parameters defining the sound is obtained by fitting the recorded signal with the expression given in relation (12). To do so, we used a signal processing approach that consists of identifying the parameters of a linear filter by auto regressive and moving average (ARMA) analysis. We model the original signal as the output of a generic linear filter whose z transform is written

$$H(z) = \frac{\sum_{m=0}^{M} a_m z^{-m}}{1 + \sum_{n=1}^{N} b_n z^{-n}} = a_0 z^{N-M} \frac{\prod_{m=1}^{M} (z - z_{0m})}{\prod_{n=1}^{N} (z - z_{pn})},$$

where z_{0m} are the zeros and z_{pn} are the poles of the system. Only the most prominent spectral components were modeled by $H(z)$. These spectral components were determined within a 50 dB amplitude dynamic, the reference being the amplitude of the most prominent spectral peak. Hence, the number of poles N and zeros M of the linear ARMA filter is determined by the number of spectral components taken into account. The coefficients a_m and b_n are estimated using classical techniques such as Steiglitz-McBride (Steiglitz and McBride, 1965). The synthesis parameters corresponding to the amplitudes, frequencies, and damping coefficients of the spectral components are thus determined:

$$\begin{cases} A_n = |H(z_{pn})|, \\ \omega_n = \arg(z_{pn}) f_s, \\ \alpha_n = \log(|z_{pn}|) f_s, \end{cases} \tag{13}$$

where f_s is the sampling frequency. In addition to the synthesis model described above, we have taken into account the attack time. Actually, even though the rising time of the sounds is very short, it does influence the perception of the sounds. These rising times were estimated on the original sounds and were reproduced by multiplying the beginning of the synthetic signal by an adequate linear function. Synthesis sounds were evaluated by informal listening tests confirming that their original sound qualities were preserved. The synthesis quality was further confirmed by results from the professional instrument maker showing a similar classification of original and synthetic sounds (classifications Cl and C2, see Sec. VI A 1).

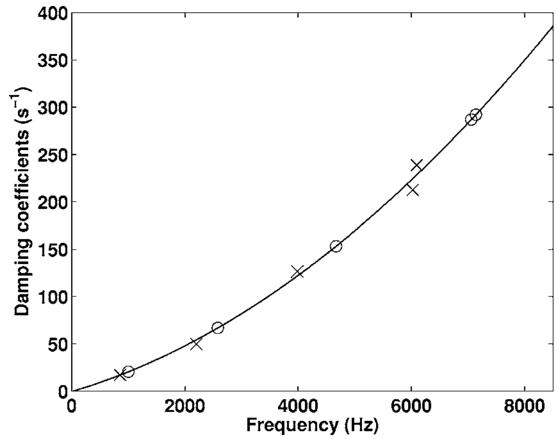

FIG. 4. The damping coefficients of the original sound (×) are fitted by a parabolic function (solid curve). The damping coefficients of the tuned sound (∘) are determined according to this damping law.

C. Tuning the sounds

The processing of tuning the sounds at the same pitch was based on some assumptions specific to the investigated stimulus set and consistent with the vibratory behavior of the bar. For the kind of sounds we are dealing with (impacted wooden bars), we assume the pitch to be related to the frequency of the first vibration mode, which is correlated with the length of the bar [cf. Eq. (8)]. Actually, if the length L changes to βL, then ω_n changes to ω_n / β^2. As a consequence, a change in pitch corresponds to a dilation of the frequency components. These assumptions made it possible to virtually equalize the pitches of the recorded bank of sounds. To minimize the pitch deviation, the whole set of sounds was tuned by transposing the fundamental frequencies to 1002 Hz, which is the mean fundamental frequency of all the sounds. The amplitude of the spectral components was kept unchanged by the tuning process. Once again, no precise listening test was performed, but our colleagues found the synthesis sounds preserved the specificity of the material.

According to the discussion in III A 1, the damping is proportional to the square of the frequency. Thus, from the expression (10), a damping law can be defined by a parabolic function that can be written in a general form:

$$\alpha(\omega) = D_A \omega^2 + D_B \omega + D_C. \tag{14}$$

As a consequence, when the pitch is changed, the damping coefficient of each tuned frequency component has to be evaluated according to the damping law measured on the original sound (cf. Fig. 4).

Figure 5 shows the comparison between the spectrum of a measured signal and the spectrum of a tuned signal after the resynthesis process. The entire sound data bank is available at http://www.lma.cnrs-mrs.fr/~kronland/JASA_Xylophone/sounds.html.

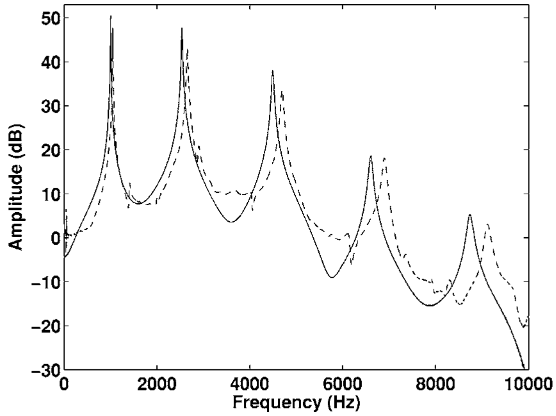

FIG. 5. Comparison between a spectrum of a measured signal (dashed trace) and the spectrum of the associated tuned signal (solid trace).

IV. EXPERIMENTAL PROTOCOL

Sounds from different wooden bars were evaluated focusing on the perceived musical quality of the wood samples. The participant was placed in front of a computer screen on which the sounds (all represented as identical crosses) were randomly distributed. The participant was asked to place the sounds on a bidimensional computer display. In particular, he was told that the horizontal dimension of the display represented an axis of musical quality so that sounds judged as having the worst/best quality were to be placed on the leftmost/rightmost part of the display. The participant could listen to the sounds as often as he wanted by simply clicking on the cross. The tests were carried on a laptop Macintosh equipped with a Sony MDR CD550 headset.

For this study, one instrument maker specialized in xylophone manufacture carried the task. For a complete perceptual study, more participants would, of course, be needed. As a first step we aimed at presenting a new methodology for an interdisciplinary approach uniting instrument makers and specialists within acoustics, signal processing, and wood sciences.

Three tests were conducted using this experimental protocol. The instrument maker carried the classification with the original sounds (recorded sounds with different pitches), called C1 (Brancheriau *et al.*, 2006a; Brancheriau *et al.*, 2006b). A second classification, called C2, using the synthesized sounds (resynthesis of the original sounds with different pitches) was done two years later. The comparison of C1 and C2 allowed us to check the quality of the resynthesis as well as the reliability of our experimental participant. The third test (C3) was carried on the signals tuned to the same pitch. The xylophone maker was not aware of the synthetic nature of sounds in C2 and C3. In particular, he was told that, for classification C3, the same pieces of wood had been sculpted in order to tune the sounds to the same fundamental frequency. Classification C3 is presented in Table III.

V. DESCRIPTORS

A. Mechanical descriptors

The wood species used for this study have been intensively examined at CIRAD and their anatomical and physical characteristics are well known. Thus, the mechanical descriptors are defined by the mass density, ρ, the longitudinal modulus of elasticity, E_ℓ, and the transverse shear modulus, G_t. The descriptors E_ℓ and G_t can be calculated using Timoshenko's model and the Bordonné solutions (Brancheriau and Baillères, 2002). We have also considered the specific longitudinal modulus, E_ℓ/ρ, and the specific shear modulus, G_t/ρ.

B. Signal descriptors

To characterize the sounds from an acoustical point of view, we calculated the following timbre descriptors (Caclin *et al.*, 2005; McAdams *et al.*, 1995): attack time, AT (the way the energy rises during the onset of the sound), spectral bandwidth, SB (spectrum spread), spectral centroid, SCG (brightness), and spectral flux, SF (the way the sound vanishes).

The attack time, AT, a temporal descriptor, characterizes the signal onset and describes the time it takes for the signal to reach its maximum. It is generally estimated as the time it takes the signal to deploy its energy from 10% to 90% of the maximum. The spectral timbre descriptors characterize the organization of the spectral peaks resulting from the modal behavior of the bar vibration. One of the most well known is the spectral centroid, SCG, which is correlated with the subjective sensation of brightness (Beauchamps, 1982):

$$\mathrm{SCG} = \frac{\sum_k f(k)|\hat{s}(k)|}{\sum_k |\hat{s}(k)|}, \tag{15}$$

where $\hat{s}$ is the discrete Fourier transform of the signal $s(t)$ and f the frequency. The spectral bandwidth, SB, measures the spread of the spectral components around the spectral centroid and is defined as (Marozeau, de Cheveigné, McAdams and Winsberg, 2003)

$$\mathrm{SB} = \sqrt{\frac{\sum_k |\hat{s}(k)|(f(k)-\mathrm{SCG})^2}{\sum_k |\hat{s}(k)|}}. \tag{16}$$

Finally, the fourth classical timbre descriptor called the spectral flux, SF, is a spectro-temporal descriptor that measures the deformation of the spectrum with respect to time. In practice, the spectral flux is given by a mean value of the Pearson correlation calculated using the modulus of local spectral representations of the signal (McAdams *et al.*, 1995):

$$\mathrm{SF} = \frac{1}{N}\sum_{n=1}^{N} \frac{\langle s_n, s_{n-1}\rangle}{s_n^2 s_{n-1}^2}, \tag{17}$$

where N represents the number of frames, s_n the modulus of the local spectrum at the discrete time n, and $\langle , \rangle$ the discrete scalar product.

In addition to these well-known timbre descriptors, we propose to consider various acoustical parameters chosen as function of the specificities of the impact sounds, i.e., the amplitude ratio between the first two frequency components of the sound, noted $A_{2/1}$, and the damping and the inharmonicity descriptors. The last two parameters are described below in more detail. The damping descriptor is defined from the Eq. (14) by the set of coefficients $\{D_A, D_B, D_C\}$ traducing the sound decrease. As the damping is the only parameter responsible for the variation of the spectral representation of the signal with respect to time, this descriptor is related to the spectral flux, SF. In addition, the damping coefficients α_1 and α_2 of components 1 and 2 have been included in the list of signal descriptors. The inharmonicity characterizes the relationship between the partials and the fundamental mode. This parameter is linked with the consonance, which is an important clue in the perceptual differentiation of sounds. For each spectral component, inharmonicity is defined by

$$I(n) = \frac{\omega_n}{\omega_0} - n. \tag{18}$$

From this expression, we propose an inharmonicity descriptor defined by a set of coefficients $\{I_A, I_B, I_C\}$ obtained by fitting $I(n)$ with a parabolic function, as suggested by the calculation $I(n)$ from Eq. (8):

$$I(n) = I_A n^2 + I_B n + I_C. \tag{19}$$

VI. RESULTS

Collected behavioral data could be considered as ordinal. Nevertheless, since the task consisted in placing the sounds on a quality axis "as a function of its musical quality," the relative position of the sounds integrates a notion of perceptual distance. Moreover, the classifications do not contain two sounds with the same position and do not show categories (see Table III). It was thus decided to consider the data as providing a quantitative estimate of perceived musical quality for the wood samples, the value associated with each species being given by its abscissa from 0 (worst quality) to 10 (best quality) on the quality axis. The main interest in using quantitative scales is the possibility of constructing an arithmetic model for perceived wood quality which can be easily used to estimate the musical quality of woods (and sounds) not considered in our experiments. All the statistical analyses were conducted with SPSS software (Release 11.0.0, LEAD Technologies).

A. Qualitative analysis—Choice of the variables

1. Resynthesis quality—Robustness of the classification

Only one participant performed the classifications on the basis of his professional skill, and his judgment of sound quality was used to build reference quality scales. The xylophone maker is thus considered as a "sensor" for measuring the acoustical wood quality. The raw classifications C1 and C2 were compared using the Wilcoxon signed rank test to evaluate the resynthesis quality of the model. Moreover, this comparison allowed us to evaluate the robustness of the xylophone maker classification. No particular distribution was assumed for the classifications. The Wilcoxon test is thus appropriate for comparing the distributions of the two classifications (C1, C2). The significance value of the Wilcoxon test ($p=0.624$) for (C1, C2) indicates that classification C1 equals classification C2. There was no significant difference in the xylophone maker responses between C1 and C2.

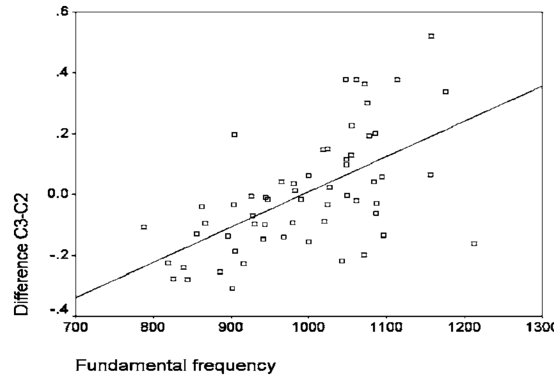

FIG. 6. Linear relationship between fundamental frequency and arithmetic difference C3-C2 ($R=0.59$, $N=59$).

2. Influence of the tuning process

The same Wilcoxon signed rank test was performed with classification C2 and classification C3 of tuned sounds. The hypothesis of equal distribution is rejected considering classifications C2 and C3. A significant difference between C2 and C3 ($p=0.001$) is due to the tuning process of sounds, which altered the sound perception of the xylophone maker. The arithmetic difference (C3-C2) was thus computed and related to the value of the fundamental frequency by using the Pearson correlation coefficient (Fig. 6). This coefficient value was found significant at the 1% level ($R=0.59$).

B. Quantitative analysis

1. Descriptor analysis

The 18 parameters presented in Table I were estimated for the tuned sounds and using standard mechanical calibrations. They are grouped into mechanical/physical descriptors and signal descriptors. In practice, for the spectral descriptors, the Fourier transform was estimated using a fast Fourier transform (FFT) algorithm. The length of the FFT was chosen so that it matches the longest sound, i.e., 2^{16} samples. For the SF calculation, the number of samples was 256 with an overlap of 156 samples. A Hamming window was used to minimize the ripples. Mechanical descriptors are linked with the intrinsic behavior of each sample but also linked with signal descriptors, as shown in Fig. 7. Indeed, the bivariate coefficients of determination matrix calculated on the basis of the 18 characteristic parameters revealed close collinearity between the parameters. Considering the strong relationship between the parameters, the statistical analyses were conducted by grouping the mechanical/physical descriptors and the signal descriptors in order to find those that best explain the classification C3.

A principal component analysis was thus conducted (Table II). Principal components analysis finds combinations of variables (components) that describe major trends in the data. This analysis generated a new set of parameters derived from the original set in which the new parameters (principal

TABLE I. Mechanical and signal descriptors computed from dynamic tests.

	No.	Variable	Signification
Mechanical descriptors	1	ρ	Mass density (kg/m^3)
	2	E_ℓ	Longitud. modulus of elasticity (MPa)
	3	G_t	Shear modulus (MPa)
	4	E_ℓ/ρ	Specific longitudinal modulus
	5	G_t/ρ	Specific shear modulus
Signal descriptors	6	$A_{2/1}$	Amplitude ratio of mode 2 and 1
	7	α_1	Temporal damping of mode 1 (s^{-1})
	8	α_2	Temporal damping of mode 2 (s^{-1})
	9	SCG	Spectral centroid (Hz)
	10	SB	Spectral bandwidth (Hz)
	11	SF	Spectral flux
	12	AT	Attack time (ms)
	13	D_A	Coefficient D_A of $\alpha(\omega)$
	14	D_B	Coefficient D_B of $\alpha(\omega)$
	15	D_C	Coefficient D_C of $\alpha(\omega)$
	16	I_A	Coefficient I_A of $I(n)$
	17	I_B	Coefficient I_B of $I(n)$
	18	I_C	Coefficient I_C of $I(n)$

components) were not correlated and closely represented the variability of the original set. Each original parameter was previously adjusted to zero mean and unit variance so that eigenvalues could be considered in choosing the main factors. In this case, the eigenvalues sum the number of variables, and eigenvalues can be interpreted as the number of original variables represented by each factor. The principal components selected thus corresponded to those of eigenvalue superior or equal to unity. Table II shows that six principal components accounted for 87% of all information contained in the 18 original parameters.

The relationships between original variables and principal components are presented in Figs. 8(a) and 8(b). These figures display the bivariate coefficient of determination between each principal component and each original parameter; the bivariate coefficient corresponds to the square loading coefficient in this analysis. The variance of the inharmonicity coefficients $\{I_A, I_B, I_C\}$ and the damping coefficients $\{D_A, D_B, D_C\}$ are captured by the first principal component and to a lesser degree by the third component [Fig. 8(a)]. The damping coefficients (α_1 and α_2), however, are mainly linked with the second component. This component is also linked with the amplitude ratio $A_{2/1}$ and with the timbre descriptors (SCG, SB, SF, AT). The variance of the mechanical/physical descriptors is scattered between all the principal components (parameter 1 is linked with PC1 and 2; parameter 2 with PC1 and 4; parameter 3 with PC3 and 5; parameter 4 with PC2, 3, and 4; and parameter 5 with PC3 and 5).

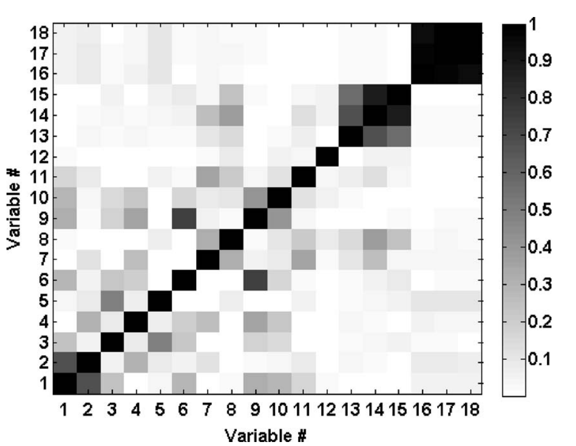

FIG. 7. Bivariate coefficients of determination for characteristic parameters ($N=59$).

2. Relationship between the descriptors and the acoustic classification of tuned sounds

a. Bivariate analysis. Figure 9 presents the results of bivariate analysis between characteristic parameters and classification C3. Assuming a linear relationship, the parameter α_1 (temporal damping of mode 1) appeared to be the best individual predictor with a R^2 value of 0.72. The second most significant predictor was the spectral flux, SF, with a R^2 value of 0.38. The other parameters were of minor importance considering classification C3. Note that the only mechanical parameter of interest was E_ℓ/ρ (specific longitudinal modulus) with a relatively low R^2 value of 0.25. Furthermore, the mass density, ρ, was not reflected in the acoustic classification (no significant R^2 value at the 1% level). Light woods and heavy woods were thus not differ-

TABLE II. Variance explained by the principal components (number of initial variables=18, number of samples=59).

Component	Eigen val.	% of Var.	Cumul. (%)
I	4.0	22.5	22.5
II	3.9	21.9	44.3
III	3.5	19.3	63.7
IV	1.8	10.1	73.8
V	1.2	6.7	80.5
VI	1.1	6.1	86.6

TABLE III. Botanical names of wood species (N=59), their density (kg/m^3), α_1 the temporal damping of mode 1(s^{-1}), SB the spectral bandwidth (Hz) and classification C3 by the xylophone maker (normalized scale from 0 to 10).

Botanical name	Density (kg/m^3)	α_1(s^{-1})	SB (Hz)	C3
Pericopsis elata Van Meeuw	680	21.76	2240	5.88
Scottellia klaineana Pierre	629	23.97	2659	6.38
Ongokea gore Pierre	842	26.07	2240	5.15
Humbertia madagascariensis Lamk.	1234	28.84	3820	0.48
Ocotea rubra Mez	623	23.47	2521	5.42
Khaya grandifoliola C.DC.	646	33.02	2968	0.95
Khaya senegalensis A. Juss.	792	33.98	3101	0.33
Coula edulis Baill.	1048	27.6	2674	2.1
Tarrietia javanica Bl.	780	20.33	2198	9.15
Entandrophragma cylindricum Sprague	734	30.6	2592	1.12
Afzelia pachyloba Harms	742	20.56	2048	8.24
Swietenia macrophylla King	571	20.99	1991	9.22
Aucoumea klaineana Pierre	399	32.17	2275	1.81
Humbertia madagascariensis Lamk	1277	23.36	3171	3.48
Faucherea thouvenotii H. Lec.	1061	20.18	2512	6.05
Ceiba pentandra Gaertn.	299	29.16	2396	2.57
Letestua durissima H. Lec.	1046	19.56	2770	3.87
Monopetalanthus heitzii Pellegr.	466	23.98	2344	5.57
Commiphora sp.	390	16.52	1269	9.77
Dalbergia sp.	916	14.29	2224	9.79
Hymenolobium sp.	600	20.58	2402	7.86
Pseudopiptadenia suaveolens Brenan	875	20.8	1989	6.53
Parkia nitida Miq.	232	26.86	1440	5.75
Bagassa guianensis Aubl.	1076	20.68	2059	6.82
Discoglypremna caloneura Prain	406	34.27	1506	1.38
Brachylaena ramiflora Humbert	866	21.85	2258	4.71
Simarouba amara Aubl.	455	21.26	1654	9.37
Gossweilerodendron balsamiferum Harms	460	35.26	1712	1.08
Manilkara mabokeensis Aubrev.	944	23.89	1788	3.25
Shorea-rubro squamata Dyer	569	23.9	1604	6.75
Autranella congolensis A. Chev.	956	38.97	3380	0.35
Entandrophragma angolense C. DC.	473	22.79	1612	7.67
Distemonanthus benthamianus Baill.	779	19.77	2088	8.75
Terminalia superba Engl. & Diels	583	21.89	2004	9.32
Nesogordonia papaverifera R.Cap.	768	27.96	2097	2.37
Albizia ferruginea Benth.	646	24.71	2221	4.32
Gymnostemon zaizou. Aubrev. & Pellegr.	380	30.15	2130	1.83
Anthonotha fragrans Exell & Hillcoat	777	24.87	1926	4.2
Piptadeniastrum africanum Brenan	975	22.41	3226	3.68
Guibourtia ehie J. Leon.	783	26.36	2156	4.05
Manilkara huberi Standl.	1096	35.11	2692	0.77
Pometia pinnata Forst.	713	25.5	1835	6.23
Glycydendron amazonicum Ducke	627	20.41	2292	7.91
Cunonia austrocaledonica Brong. Gris.	621	31.05	3930	0.59
Nothofagus aequilateralis Steen.	1100	37.76	3028	0.18
Schefflera gabriellae Baill.	570	28.16	1872	1.42
Gymnostoma nodiflorum Johnst.	1189	33	3013	1.26
Dysoxylum sp.	977	23.85	2106	4.49
Calophyllum caledonicum Vieill.	789	19.82	2312	8.66
Gyrocarpus americanus Jacq.	206	38.39	1982	0.6
Pyriluma sphaerocarpum Aubrev.	793	30.83	2318	1.23
Cedrela odorata L.	512	30.45	2070	3
Moronobea coccinea Aubl.	953	21.67	1781	4.92
Goupia glabra Aubl.	885	45.61	2525	0.22
Manilkara huberi Standl.	1187	22.6	2917	2.78
Micropholis venulosa Pierre	665	22.51	3113	7.12
Cedrelinga catenaeformis Ducke	490	22.5	1626	7.31
Vouacapoua americana Aubl.	882	23.18	1986	6.88
Tarrietia Densiflora Aubrev & Normand	603	29.76	2326	1.62

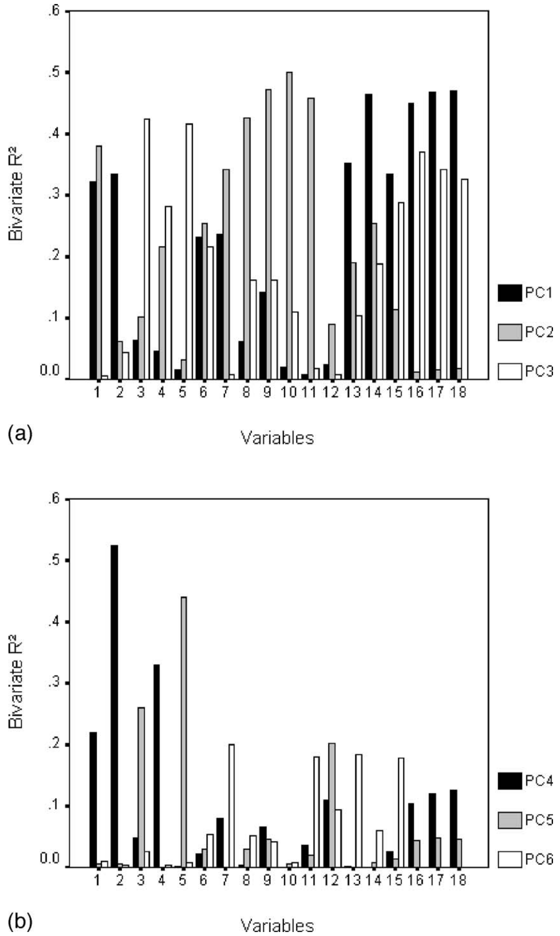

FIG. 8. Bivariate determination coefficient between original variables and principal components: (a) for PC1, PC2 and PC3; (b) for PC4, PC5 and PC6.

entiated by the xylophone maker in the acoustic classification.

b. Multivariate linear regression analysis. The second step of the analysis was to build a robust linear model to take into account the most significant predictors. The robustness of the model assumes that no multicollinearity among the variables exists (Dillon and Goldstein, 1984). The stepwise selection method was thus used to perform multivariate

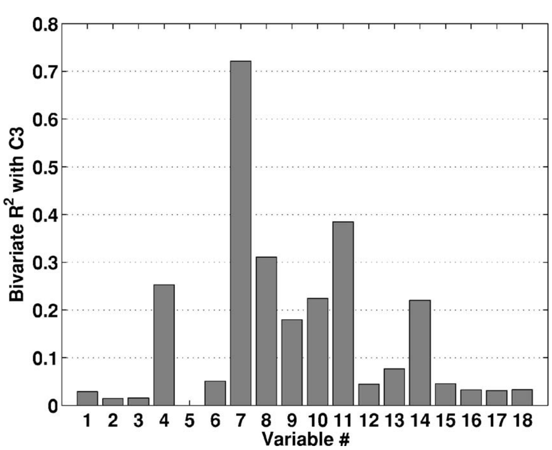

FIG. 9. Bivariate coefficients of determination between characteristic parameters and classification C3 (N=59).

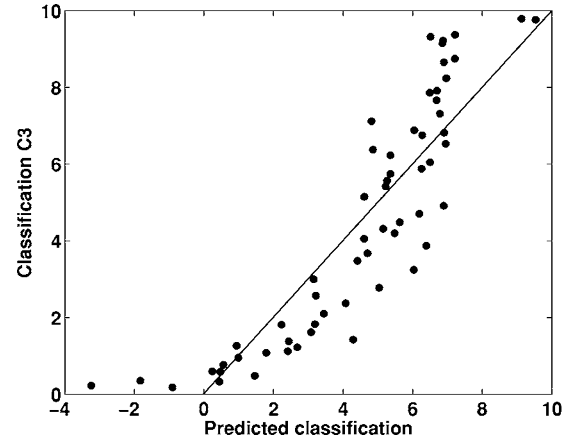

FIG. 10. Predicted vs observed C3 classification (linear predictors α_1 and SB, R^2=0.77, N=59).

analysis. This method enters variables into the model one by one and tests all the variables in the model for removal at each step. Stepwise selection is designed for the case of correlations among the variables. Other automatic selection procedures exist (forward selection and backward elimination, for example), and the models obtained by these methods may differ, especially when independent variables are highly intercorrelated. Because of the high correlation between variables, several regression models almost equally explain classification C3. However, stepwise selection was used to build one of the most significant models with noncorrelated variables relating to different physical phenomena.

The final linear model obtained by stepwise variable selection included the two predictors, α_1 and SB. The predicted classification is given by:

$$\hat{C}3_{\text{Linear}} = -3.82 \times 10^{-1}\alpha_1 - 1.32 \times 10^{-3}SB + 17.52. \quad (20)$$

The multiple coefficient of determination was highly significant (R^2=0.776 and Adjusted R^2=0.768, Fig. 10) and each regression coefficient was statistically different from zero (significance level: 1%). The predictor α_1 was predominant in the model with a partial coefficient value of $R_{\alpha 1}$= −0.84 (R_{SB}=−0.44). The negative sign of $R_{\alpha 1}$ showed that samples with high damping coefficients were associated with a poor acoustic quality.

Partial least squares regression showed that the damping coefficient α_1 was predominant in the model (Brancheriau *et al.*, 2006b). However, the physical significance of the partial least squares model was difficult to explain because the original variables were grouped in latent variables. The stepwise procedure was thus used to better understand the regression results.

The multivariate analysis differed from the bivariate analysis by the replacement of SF by SB, because the selected set of predictors was formed by noncorrelated variables. SB was thus selected because of the low correlation between α_1 and SB with a coefficient value of $R_{\alpha 1/\text{SB}}$=0.29 instead of SF with a value of $R_{\alpha 1/\text{SF}}$=−0.60.

Principal components regression (PCR) was another way to deal with the problem of strong correlations among the variables. Instead of modeling the classification with the variables, the classification was modeled on the principal component scores of the measured variables (which are orthogonal and therefore not correlated). The PCR final model was highly significant with a multiple R^2 value of 0.741 and Adjusted R^2 value of 0.721. Four principal components were selected and the resulting scatter plot was similar to the one in Fig. 10. Comparing the two multivariate models, we found the PCR model to be less relevant than the stepwise one. The R^2 of the PCR model was indeed lower than the R^2 of the stepwise model. Furthermore, the PCR model included four components while only two independent variables were included in the stepwise model. The difference between these two models was explained by the fact that the whole information contained in the characteristic parameters (Table I) was not needed to explain the perceptual classification. The PCR procedure found components that capture the greatest amount of variance in the predictor variables, but did not build components that both capture variance and achieve correlation with the dependent variable.

c. Multivariate nonlinear regression analysis. The configuration of points associated with the linear model (C3, α_1 and SB) in Fig. 10 indicated a nonlinear relationship. This was particularly true for samples of poor acoustic quality (negative values of the standardized predicted classification). As a final step of the analysis, we built a nonlinear model of the behavioral response. In particular, we transformed the values predicted by the linear model $\hat{C}3_{\text{Linear}}$ using a sigmoidal transform. Such transform was consistent with the relationship between C3 and $\hat{C}3_{\text{Linear}}$ (see Fig. 10). The fitting coefficients were extracted via the Levenberg-Marquardt optimization procedure by minimizing the residual sum of squares (dependent variable C3 and independent variable $\hat{C}3_{\text{Linear}}$: predicted classification with the linear modeling). The final equation is written as follows:

$$\hat{C}3_{\text{sigmoid}} = \frac{10}{1 + e^{-\frac{\hat{C}3_{\text{Linear}}-5}{1.64}}} \qquad (21)$$

with $\hat{C}3_{\text{Linear}}$ defined by Eq. (20). The multiple coefficient of determination was highly significant (R^2=0.82) and each nonlinear regression coefficient was statistically different from zero (significance level: 1%). The nonlinear model provided a better fit than the linear model; moreover no apparent systematic feature appeared, indicating that residuals were randomly distributed (Fig. 11).

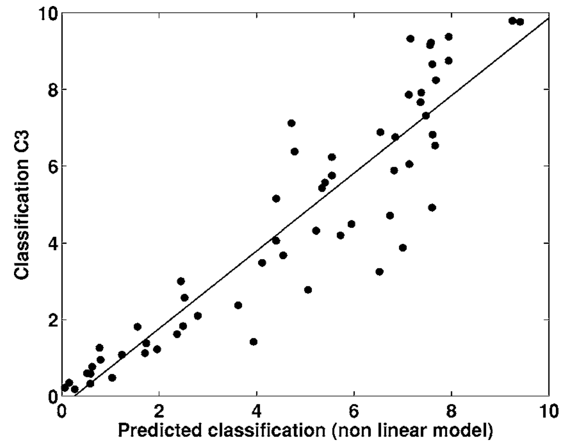

FIG. 11. Predicted vs observed C3 classification (nonlinear predictors α_1 and SB, R^2=0.82, N=59).

VII. DISCUSSION

In this section, we discuss the main results presented above, attempting to better understand the sound descriptors' influence on the xylophone maker classification. Further on, we discuss the influence of the pitch and the relationship between the wood anatomy and the produced sounds.

A. On the reliability of the xylophone maker

As we pointed out in the introduction, this paper does not aim to give categorical clues for choosing interesting species of wood for xylophone manufacturing. Nevertheless, note that these first conclusions probably accurately reflect what xylophone makers look for. Although we tested our methodology with only one renowned xylophone maker, the results show that:

- In accordance with the xylophone maker community, our maker chose *Dalbergia* sp. as the best species. Moreover, this choice was confirmed on both tuned and original sound classifications.
- The comparison of classifications C1 and C2 showed no significant differences according to the Wilcoxon test.

These observations confirm the good reliability of our xylophone maker and the accuracy of the results, which were further informally confirmed by both instrument makers and musicians.

B. Relation between descriptors and wood classification

The classification by the xylophone maker is correlated with several descriptors. Those that play an important role are three descriptors related to the time course of the sound (α_1, α_2 and SF) and two descriptors related to the spectral content of the sound (SCG and SB). Note that the physical descriptors linked with the wood properties do not explain by themselves the classification of the instrument maker, even though E_ℓ/ρ seems to be the most pertinent one. The relatively low importance of the specific modulus regarding classification C3 could be explained by its high correlation with the fundamental frequency (R^2=0.91) and its low correlation with the temporal damping coefficient α_1 (R^2=0.26). Most of the descriptors are correlated; these correlations are coherent with the physics and are shown in a qualitative way in Fig. 7. Both coefficients of the polynomial decomposition of $\alpha(\omega)$ are strongly correlated. So are the coefficients of the polynomial decomposition of $I(n)$. This finding points out the relative consistency in the behavior of the damping and the inharmonicity laws with respect to the species. Parameters α_1 and α_2 are also correlated, showing the monotonic behavior of the damping with respect to the frequency: the higher the frequency, the higher the damping. As a consequence, both α_1 and α_2 are correlated with the spectral flux, SF, since these descriptors are the only ones that relate to the time course of the sound.

Both global spectral descriptors, SCG and SB, are also correlated, showing that their increase is strongly related to the adjunction of high frequency energy. These descriptors are in addition correlated with the ratio $A_{2/1}$ and with the physical descriptors ρ and E_ℓ/ρ. This correlation can be explained by the way the energy is distributed through the excited modes. Actually, assuming that the bars are impacted identically (good reproducibility of the impact in the experimental setup), the initial energy injected depends on the impedance of each bar. Since the bars were impacted in the transversal direction, one can assume that the transversal Young modulus of elasticity together with the mass density are the main parameters in the difference of amplitudes of modes 1 and 2.

The multivariate linear regression analysis highlighted two main descriptors: α_1 and SB. These descriptors are noncorrelated and give rise to a linear predictor of the classification $\hat{C}3_{\mathrm{Linear}}$ that explains 77% of the variance. This model is of great importance in the choice of species. Actually, it emphasizes the fact that the xylophone maker looks for a highly resonant sound (the coefficient of α_1 is negative) containing a few spectral components (the coefficient of SB is also negative). Such a search for a crystal-clear sound could explain the general choice of *Dalbergia* sp., which is the most resonant species and the most common in xylophone bars. Indeed, the predominance of α_1 agrees with the first rank of *Dalbergia* sp., for which $\alpha_1 = 14.28\ \mathrm{s}^{-1}$ is the smallest in the data bank ($14.28\ \mathrm{s}^{-1} < \alpha_1 < 45.61\ \mathrm{s}^{-1}$) and SB $=2224$ Hz is medium range in the data bank ($1268\ \mathrm{Hz} < \mathrm{SB} < 3930\ \mathrm{Hz}$). Holz (1996) showed that the damping factor value α_1 should be lower than about $30\ \mathrm{s}^{-1}$ for a fundamental frequency value of 1000 Hz, which corresponds to the mean value of the study. The average value of α_1 is indeed $26.13\ \mathrm{s}^{-1}$ with a standard deviation of $6.18\ \mathrm{s}^{-1}$. Actually, xylophone makers use a specific way of carving the bar by removing substance in the middle (Fletcher and Rossing, 1998). This operation tends to minimize the importance of partial 2, decreasing both the SCG and the SB. The importance of α_1 in the model is in line with several studies showing that the damping is a pertinent clue in the perception of impacted materials (Klatzky *et al.*, 2000; Wildes and Richards, 1988). Concerning parameter SB, the spectral distribution of energy is also an important clue, especially for categorization purposes.

The linear classification prediction has been improved by taking into account nonlinear phenomena. The nonlinear model then explains 82% of the variance. The nonlinear relationship between the perceptual classification and predictors (α_1 and SB) was explained by the instrument maker's strategy during the evaluation of each sample. The xylophone maker proceeded by first identifying the best samples and then the worst samples. This first step gave him the upper and lower bounds of the classification. The final step was to sort the samples of medium quality and place them between the bounds. One could deduce that three groups of acoustic quality (good, poor, and medium quality) were formed before the classification and that inside these groups the perceptual distance between each sample was different. The sigmoid shape indicated that the perceptual distance was shorter for good and poor quality groups than for medium quality groups. As a consequence, the nonlinear model is probably linked with the way the maker proceeded and cannot be interpreted as an intrinsic model for wood classification. Another explanation for the nonlinear relationship can also be found in the nonlinear transform relating physical and perceptual dimensions.

Note finally that there was no correlation between the classification and the wood density. However it is known that the wood density is of great importance for instrument makers. Holz (1996) suggested that the "ideal" xylophone wood bars would have density values between 800 and 950 $\mathrm{kg/m}^3$. This phenomenon is due to the way we designed our experimental protocol, focusing on the sound itself and minimizing multi-sensorial effects (avoiding the access to visual and tactile information). Actually, in a situation where the instrument maker has access to the wood, bars with weak density are rejected for manufacturing and robustness purposes, irrespective of their sound quality.

C. Influence of the fundamental frequency (pitch) on the classification

As discussed previously, timbre is a key feature for appreciating sound quality and it makes it possible to distinguish tones with equal pitch, loudness, and duration (ANSI, 1973). Since this study aims at better understanding which timbre descriptor is of interest for wood classification, one expected differences in the classification of the tuned and the original sound data banks. The difference between classifications C2 (various pitches) and C3 (same pitches) shows a clear linear tendency; it is represented in Fig. 6 as a function of the original fundamental frequency of the bars. The difference is negative (respectively positive) for sounds whose fundamental frequencies are lower (respectively higher) than the mean frequency. The Pearson coefficient associated with the linear relationship between the arithmetic difference of the classification and the fundamental frequency leads to the important observation that *a wooden bar with a low fundamental frequency tends to be upgraded while a wooden bar with a high fundamental frequency tends to be downgraded*. This finding agrees with our linear prediction model, which predicts weakly damped sounds would be better classified than highly damped ones. Actually, sounds with low (respectively high) fundamental frequencies were transposed toward high (respectively low) frequencies during the tuning process, implying α_1 increase (respectively decrease), since the damping is proportional to the square of the frequency (cf. Sec. III C). As an important conclusion, one may say that the instrument maker cannot judge the wood itself independently of the bar dimensions, since the classification is influenced by the pitch changes, favoring wood samples generating low fundamental frequency sounds.

Once again, note the good reliability of our instrument maker, who did not change the classification of sounds whose fundamental frequency was close to the mean fundamental frequency of the data bank (i.e., sounds with nearly unchanged pitch). Actually, the linear regression line passes close to 0 at the mean frequency 1002 Hz. Moreover, the *Dalbergia* sp. was kept at the first position after the tuning process, suggesting that no dramatic sound transformations had been made. In fact, this sample was transposed upwards by 58 Hz, changing α_1 from 13.6 s^{-1} to 14.28 s^{-1}, which still was the smallest value of the tuned data bank.

D. Relationship between wood anatomy and perceived musical quality

The damping α_1 of the first vibrational mode was an important descriptor explaining the xylophone maker classification. Equation (11) shows that this descriptor is related to the quality factor Q, and consequently to the internal friction coefficient tan ϕ (inverse of the quality factor Q), which depends on the anatomical structure of the wood. An anatomical description of the best classified species has been discussed in a companion article (Brancheriau *et al.*, 2006b). We briefly summarize the main conclusions and refer the reader to the article for more information. A draft anatomical portrait of a good acoustic wood could be drawn up on the basis of our analysis of wood structures in the seven acoustically best and seven poorest woods. This portrait should include a compulsory characteristic, an important characteristic, and two or three others of lesser importance. The key trait is the axial parenchyma. It should be paratracheal, and not very abundant if possible. If abundant (thus highly confluent), the bands should not be numerous. Apotra-cheal parenchyma can be present, but only in the form of well-spaced bands (e.g., narrow marginal bands). The rays (horizontal parenchyma) are another important feature. They should be short, structurally homogeneous but not very numerous. The other characteristics are not essential, but they may enhance the acoustic quality. These include:

- Small numbers of vessels (thus large);
- A storied structure;
- Fibers with a wide lumen (or a high flexibility coefficient, which is the ratio between the lumen width and the fiber width; it is directly linked with the thickness of the fiber).

These anatomical descriptions give clues for better choosing wood species to be used in xylophone manufacturing. They undoubtedly are valuable for designing new musical materials from scratch, such as composite materials.

VIII. CONCLUSION

We have proposed a methodology associating analysis-synthesis processes and perceptual classifications to better understand what makes the sound produced by impacted wooden bars attractive for xylophone makers. This methodology, which focused on timbre-related acoustical properties, requires equalization of the pitch of recorded sounds. Statistical analysis of the classifications made by an instrument maker highlighted the importance of two salient descriptors: the damping of the first partial and the spectral bandwidth of the sound, indicating he searched for highly resonant and crystal-clear sounds. Moreover, comparing the classifications of both the original and processed sounds showed how the pitch influences the judgment of the instrument maker. Indeed, sounds with originally low (respectively high) fundamental frequency were better (lesser) classified before the tuning process than after. This result points to the preponderance of the damping and reinforces the importance of the pitch manipulation to better dissociate the influence of the wood species from that of the bar geometry. Finally, the results revealed some of the manufacturers' strategies and pointed out important mechanical and anatomical characteristics of woods used in xylophone manufacturing. From a perceptual point of view, the internal friction seems to be the most important characteristic of the wood species. Nevertheless, even though no correlation has been evidenced between the classification and the wood density, it is well known that this parameter is of great importance for instrument makers as evidence of robustness. As mentioned in the introduction, this work was the first step towards determining relations linking sounds and wood materials. Future works will aim at confirming the results described in this paper by taking into account classifications made by other xylophone makers in the statistical analysis. We plan to use this methodology on a new set of wood species having mechanical and anatomical characteristics similar to those well classified in the current test. This should point out unused wood species of interest to musical instrument manufacturers and will give clues for designing new musical synthetic materials.

ACKNOWLEDGMENTS

The authors thank Robert Hébrard, the xylophone maker who performed the acoustic classification of the wood species. They are also grateful to Pierre Détienne for useful advice and expertise in wood anatomy. They also thank Bloen Metzger and Dominique Peyroche d'Arnaud for their active participation in the experimental design and the acoustical analysis, and Jérémy Marozeau who provided the graphical interface for the listening test. We would also thank the reviewers for useful suggestions.

American National Standards Institute (**1973**). *American National Standard Psychoacoustical Terminology* (American National Standards Institute, NY).

Adrien, J. M. (**1991**). *The Missing Link: Modal Synthesis* (MIT Press, Cambridge, MA), Chap. 8, pp. 269–297.

Avanzini, F., and Rocchesso, D. (**2001**). "Controlling material properties in physical models of sounding objects," in *Proceedings of the International Computer Music Conference 2001*, 17–22 September 2001, Hawana, pp. 91–94.

Beauchamps, J. W. (**1982**). "Synthesis by spectral amplitude and "brightness" matching of analyzed musical instrument tones," J. Audio Eng. Soc. **30**(6), 396–406.

Blay, M., Bourgain , and Samson (**1971**). "Application des techniques électroacoustiques à la détermination du module d'élasticité par un procédé nondestructif (Application of electroacoustic techniques to determine the elasticity modulus by nondestructive procedure)," Technical Review to Advance Techniques in Acoustical, Electrical and Mechanical Measurement **4**, 3–19.

Bork, I. (**1995**). "Practical tuning of xylophone bars and resonators," Appl. Acoust. **46**, 103–127.

Brancheriau, L., and Baillères, H. (**2002**). "Natural vibration analysis of clear wooden beams: A theoretical review," Wood Sci. Technol. **36**, 347–365.

Brancheriau, L., Baillères, H., Détienne, P., Gril, J., and Kronland-Martinet, R. (**2006a**). "Key signal and wood anatomy parameters related to the acoustic quality of wood for xylophone-type percussion instruments," J. Wood Sci. **52**(3), 270–274.

Brancheriau, L., Baillères, H., Détienne, P., Kronland-Martinet, R., and Metzger, B. (**2006b**). "Classifying xylophone bar materials by perceptual, signal processing and wood anatomy analysis," Ann. Forest Sci. **62**, 1–9.

Bucur, V. (**1995**). *Acoustics of Wood* (CRC Press, Berlin).

Caclin, A., McAdams, S., Smith, B. K., and Winsberg, S. (**2005**). "Acoustic correlates of timbre space dimensions: A confirmatory study using synthetic tones," J. Acoust. Soc. Am. **118**(1), 471–482.

Chaigne, A., and Doutaut, V. (**1997**). "Numerical simulations of xylophones. I. Time-domain modeling of the vibrating bars," J. Acoust. Soc. Am. **101**(1), 539–557.

Dillon, W. R., and Goldstein, M. (**1984**). *Multivariate Analysis—Methods and Applications* (Wiley, New York).

Doutaut, V., Matignon, D., and Chaigne, A. (**1998**). "Numerical simulations of xylophones. II. Time-domain modeling of the resonator and of the radiated sound pressure," J. Acoust. Soc. Am. **104**(3), 1633–1647.

Fletcher, N. H., and Rossing, T. D. (**1998**). *The Physics of Musical Instruments*, 2nd ed. (Springer-Verlag, Berlin).

Giordano, B. L., and McAdams, S. (**2006**). "Material identification of real impact sounds: Effects of size variation in steel, wood, and Plexiglass plates," J. Acoust. Soc. Am. **119**(2), 1171–1181.

Graff, K. F. (**1975**). *Wave Motion in Elastic Solids* (Ohio State University Press), pp. 100–108.

Holz, D. (**1996**). "Acoustically important properties of xylophon-bar materials: Can tropical woods be replaced by European species?" Acust. Acta Acust. 82(6), 878–884.

Klatzky, R. L., Pai, D. K., and Krotkov, E. P. (**2000**). "Perception of material from contact sounds," Presence: Teleoperators and Virtual Environments **9**(4), 399–410.

Lutfi, R. A., and Oh, E. L. (**1997**). "Auditory discrimination of material changes in a struck-clamped bar," J. Acoust. Soc. Am. **102**(6), 3647–3656.

Marozeau, J., de Cheveigné, A., McAdams, S., and Winsberg, S. (**2003**). "The dependency of timbre on fundamental frequency," J. Acoust. Soc. Am. **114**, 2946–2957.

Matsunaga, M., and Minato, K. (**1998**). "Physical and mechanical properties required for violin bow materials II. Comparison of the processing properties and durability between pernambuco and substitutable wood species," J. Wood Sci. **44**(2), 142–146.

Matsunaga, M., Minato, K., and Nakatsubo, F. (**1999**). "Vibrational property changes of spruce wood by impregnating with water-soluble extractives of pernambuco (*Guilandina echinata Spreng*.)," J. Wood Sci. **45**(6), 470–474.

Matsunaga, M., Sugiyama, M., Minato, K., and Norimoto, M. (**1996**). "Physical and mechanical properties required for violin bow materials," Holzforschung **50**(6), 511–517.

McAdams, S., Chaigne, A., and Roussarie, V. (**2004**). "The psychomechanics of simulated sound sources: Material properties of impacted bars," J. Acoust. Soc. Am. **115**(3), 1306–1320.

McAdams, S., Winsberg, S., Donnadieu, S., Soete, G. D., and Krimphoff, J. (**1995**). "Perceptual scaling of synthesized musical timbres: Common dimensions, specificities, and latent subject classes," Psychol. Res. **58**, 177–192.

Obataya, E., Umewaza, T., Nakatsubo, F., and Norimoto, M. (**1999**). "The effects of water soluble extractives on the acoustic properties of reed (*Arundo donax* L.)," Holzforschung **53**(1), 63–67.

Ono, T., and Norimoto, M. (**1983**). "Study on Young's modulus and internal friction of wood in relation to the evaluation of wood for musical instruments," Jpn. J. Appl. Phys., Part 1 **22**(4), 611–614.

Ono, T., and Norimoto, M. (**1985**). "Anisotropy of Dynamic Young's Modulus and Internal Friction in Wood," Jpn. J. Appl. Phys., Part 1 **24**(8), 960–964.

Steiglitz, K., and McBride, L. E. (**1965**). "A technique for the identification of linear systems," IEEE Trans. Autom. Control **AC-10**, 461–464.

Sugiyama, M., Matsunaga, M., Minato, K., and Norimoto, M. (**1994**). "Physical and mechanical properties of pernambuco (*Guilandina echinata* Spreng.) used for violin bows," Mokuzai Gakkaishi **40**, 905–910.

Valette, C., and Cuesta, C. (**1993**). *Mécanique de la Corde Vibrante (Mechanics of Vibrating String)*, Traité des Nouvelles Technologies, série Mécanique (Hermès, Paris).

Wildes, R. P., and Richards, W. A. (**1988**). *Recovering Material Properties from Sound* (MIT Press, Cambridge, MA), Chap. 25, pp. 356–363.